Journal of Physics: Conference Series

OPEN ACCESS

Interaction of fibrinogen and albumin with titanium dioxide nanoparticles of different crystalline phases

To cite this article: Arianna Marucco *et al* 2013 *J. Phys.: Conf. Ser.* **429** 012014

View the article online for updates and enhancements.

You may also like

- Dynamic protein adsorption at the polyurethane copolymer/water interface
M Yaseen, H J Salacinski, A M Seifalian et al.
- Fabrication of 3D-nanofibrous fibrinogen scaffolds using salt-induced self assembly
Karsten Stapelfeldt, Stephani Stamboroski, Polina Mednikova et al.
- Insoluble fibrinogen particles for harvesting and expanding attachment-dependent cells and for trapping suspended cancer cells in the presence of blood
Duha Fahham, Emmanuelle Merquiol, Tamar Gilon et al.

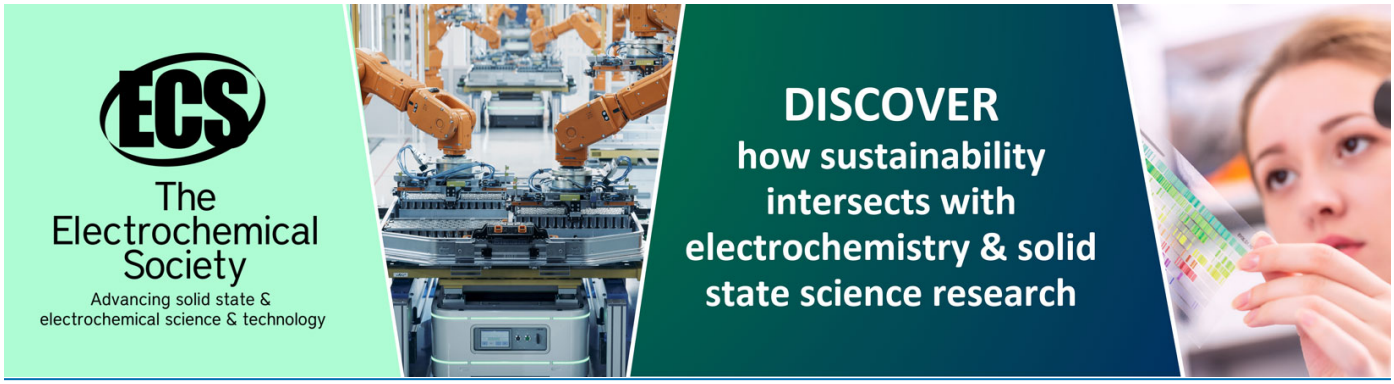

This content was downloaded from IP address 3.144.151.106 on 26/04/2024 at 08:45

Journal of Physics: Conference Series **429** (2013) 012014 doi:10.1088/1742-6596/429/1/012014

Interaction of fibrinogen and albumin with titanium dioxide nanoparticles of different crystalline phases

Arianna Marucco, Ivana Fenoglio, Francesco Turci and Bice Fubini

University of Torino, Dept. of Chemistry, Interdepartmental Centre "G. Scansetti" for Studies on Asbestos and Other Toxic Particulates and Interdepartmental Center for Nanostructured Interfaces and Surfaces, Via P. Giuria 7, 10125 Torino, Italy

ariannamaria.marucco@unito.it

Abstract. TiO_2 nanoparticles (NPs) are contained in different kinds of industrial products including paints, self-cleaning glasses, sunscreens. TiO_2 is also employed in photocatalysis and it has been proposed for waste water treatment. Micrometric TiO_2 is generally considered a safe material, while there is concern on the possible health effects of nanometric titania. Due to their small size NPs may migrate within the human body possibly entering in the blood stream. Therefore studies on the interaction of NPs with plasma proteins are needed. In fact, the interaction with proteins is believed to ultimately influences the NPs biological fate. Fibrinogen and albumin are two of the most abundant plasma proteins. They are involved in several important physiological functions. Furthermore, fibrinogen is known to trigger platelet adhesion and inflammation. For these reasons the study of the interaction between these protein and nanoparticles is an important step toward the understanding of the behavior of NPs in the body. In this study we investigated the interaction of albumin and fibrinogen with TiO_2 nanoparticles of different crystal phases (rutile and anatase) using an integrated set of techniques. The amount of adsorbed fibrinogen and albumin for each TiO_2 surface was investigated by using the bicinchoninic acid assay (BCA). The variation of the surface charge of the NP-protein conjugates respect to the naked NPs was used to indirectly estimate both surface coverage and reversibility of the adsorption upon dilution. Surface charge was monitored by measuring the ζ potential with a conventional electrophoretic light scattering (ELS) system. The extent of protein deformation was evaluated by Raman Spectroscopy. We found that both proteins adsorb irreversibly against electrostatic repulsion, likely undergoing conformational changes or selective orientation upon adsorption. The size of primary particles and the particles aggregation rather than the crystal phase modulate the affinity of fibrinogen for the TiO_2 surfaces.

1. Introduction

The rapid diffusion in the market of nanotechnological products opens new concerns on the possible adverse effects following the direct or indirect exposure of humans to nanoparticles (NPs) [1-4]. The hazard associated to nanomaterials is often difficult to be defined, because of knowledge of the interaction of nanoscale objects with living matter is still incomplete [5-7].

When a foreign body comes in contact with a biological fluid its surface is quickly covered by the components of the fluid, particularly proteins. A layer of proteins, defined as "protein corona" in the case of nanoparticles [8], is rapidly formed. Such layer is a dual system, composed by a core of strongly bound proteins and an outer layer of fast exchanging molecules [9, 10]. The composition of the protein corona depends upon a series of competitive processes driven by both thermodynamic and

kinetic factors [9]. Interaction with blood proteins is considered the most critical step among the events determining the fate of NPs in the body. At the same time the interaction with blood proteins may trigger adverse responses like thrombosis and inflammation [11]. Plasma is a very complex system composed by thousand of different proteins, the two most abundant being albumin (35-50 mg/ml) and fibrinogen (1.8-3.5 mg/ml). Albumin is a soft protein of 67 kDa exhibiting a globular shape ($9 \times 6 \times 5$ nm). At physiological pH it has a net negative charge the isoelectric point (IP) being at pH 4.8. This protein is synthetized in the liver and its main physiological role is the transport of solutes in the blood stream to their target organs. It also contributes to maintain the pH and the osmotic pressure of plasma [12].

Fibrinogen is a large and complex glycoprotein (340 kDa). It has a rod-like shape with dimensions of $9 \times 47.5 \times 6$ nm and, like albumin, it shows a negative net charge at physiological pH (IP at pH 5.2) [13]. It is synthesized in the liver and it is involved in several different biological functions such as blood clotting and stabilization of thrombi following vessel injury [14]. It also triggers foreign body reactions following implantation of prosthesis [15] and inflammatory responses to NPs [16]. These effects are mediated by surface-driven conformational changes leading to the exposure of specific epitopes when fibrinogen is adsorbed [15,16]. It is generally accepted that the physico-chemical properties of the surface play a crucial role in the interaction of a solid with living matter [15, 17, 18, 19, 20] but there is not yet a clear definition of the physico-chemical determinants of such interactions.

Here we report about the interaction of albumin and fibrinogen with three different samples of TiO_2 having different crystal phase (rutile and anatase). The study aims to elucidate the possible influence of the crystal phase on the behaviour of these two proteins at the titania surface.

Rutile and anatase nanometric titanium dioxide have been chosen for this study since they are largely used in industry mainly as UV blockers in sunscreen and plastics. TiO_2 finds also application in catalysis and has been proposed for water and air remediation thanks to its high photo-reactivity. Nanometric TiO_2 is also a promising material in nanomedicine [21]. Exposure of workers and users to this kind of nanomaterial is therefore expected to increase in the next years.

The interaction of nano- TiO_2 with the two proteins was investigated by evaluating the amount of protein interacting with the powder extent of surface coverage and irreversibility of the process (spectrophotometry and electrophoretic light scattering). The occurrence of conformational changes was also investigated by Raman spectroscopy.

2. Materials and Methods

2.1 Materials

Pyrogenic nanometric anatase/rutile powder (Aeroxide P25) ($T_{A/R}$) was purchased from Degussa-Evonik (Germany) while rutile (MT500B) (T_R) was from LCM-Trading (Italy)

Nanometric anatase powder (T_A) was synthesized by a sol gel process as described in previous work [22].

Bovine Plasma Fibrinogen (BPF) and Bovine Serum Albumin (BSA) were chosen as model for human fibrinogen and albumin and purchased from Sigma Aldrich (Germany) and used without further purification.

In all experiments, ultrapure Milli Q (Millipore, Billerca, MA) water was used. All other reagents were from Sigma Aldrich (Germany).

2.2 Methods

2.2.1 X ray diffraction

XRD spectra were collected on a diffractometer (PW1830, Philips) using CoKα radiation, in the (20−90) 2θ range, with step width 2θ = 0.05, and diffraction peaks have been indexed according to the ICDD database (International Centre for Diffraction Data). The spectra have been elaborated (X'-pert Highscore 1.0c, PANalytical B.V.) in order to assess the primary particle mean diameter of the different specimens.

2.2.2 HR-TEM investigation

The morphology of rutile nanoparticles were investigated by JEOL 3010-UHR HR-TEM equipped with a LaB6 filament operated at 300 kV, beam current 114 µA and equipped with a 2k x 2k pixels Gatan US1000 CCD camera. The nanoparticles were dispersed in ultrapure water (MilliQ system, Millipore), sonicated for 20 minutes and a droplet was deposited on lacey carbon Cu grids.

2.2.3 X ray fluorescence diffraction

The TiO_2 samples were analyzed using an EDAX Eagle III energy dispersive micro-XRF spectrometer equipped with a Rh X-ray tube and a polycapillary exciting a circular area of nominally 30 µm diameter. Data collection occurred at each point for 200 s detector live time, with X-ray tube settings adjusted for 30% dead time. About 1×10^6 Cps were counted per scan. At least 4 points were collected for each sample.

2.2.4Surface Area Measurements

The surface area of the particles was measured by means of the Brunauer, Emmett, and Teller (BET) method based on N_2 adsorption at 77 K (Micrometrics ASAP 2020).

2.2.5 ζ Potential.

The ζ Potential was evaluated by means of electrophoretic light scattering (ELS) (Zetasizer Nano-ZS, Malvern Instruments, Worcestershire, U.K.)

In this technique the velocity of particles in an oscillating electric field, which is proportional to their ζ Potential, was measured by light scattering. TiO_2 particles were suspended in ultrapure water and then sonicated for 2 min with a probe sonicator (100 W, 60 kHz, Sonoplus, Bandelin, Berlin, Germany).

The ζ Potential in function of pH was measured for all the samples; in water and in 10 mM phosphate buffer (PBS) for monitoring nanoparticles surface charge. The ζ potential at pH 7.4 was obtained by interpolation of a curve obtained by measuring the ζ potential at different pH (2−9) by adding 0.1 M HCl or NaOH to the suspension

The measurements were also repeated on titania powders incubated with protein solution and on titania powders incubated with protein and then washed three times in PBS.

2.2.6 Evaluation of the quantity of protein adsorbed on nanoparticles

Titania powders were suspended (33 mg/ml) in buffered protein solution (0.01M phosphate buffer: pH 7.4, 0.138 M NaCl and 2.7 mM KCl) at different concentrations (100-10000 mg/L).

The suspension were stirred in a thermostatic stirrer at 37°C for 1h and centrifuged at 11.000 RPM, then filtered through a membrane filter (cellulose acetate, pore diameter 0.45 µm) and the concentration of protein in the supernatant was determined spectrophotometrically (562 nm) by using the bicinchoninic acid (BCA) assay.

The amount of protein adsorbed was calculated as a difference between the final and the initial concentration of protein in the supernatant. The results are reported as the mean value of at the least three separate determinations ± standard error. The data are expressed as nano moli of protein adsorbed on m^2 as a function of the protein concentration present in solution after the incubation.

The theoretical monolayers were calculated by protein sizes as the amount needed for obtain a side-on protein monolayer on a totally available flat surface.

*2.2.7 Raman Spectroscopy***.**

Raman spectra were acquired using an integrated confocal Raman system that includes a Horiba Jobin-Yvon HR 800 microspectrometer, an Olympus BX41 microscope, and a CCD air-cooled detector operating at -70°C.

A polarized solid-state Nd laser operating at wavelength of 532.11nm and a power of 80 mW was used as excitation source.

Calibration of the instrument was performed by measuring the Stokes and the anti-Stokes bands of the Si band at 520.7 cm^{-1} .

For the powder samples the measure were made placing the sample on a polished stainless steel slide, and a 50X objective delivering a power of ca. 15 mW to the sample was used.

Spectra were acquired with a spectral resolution of ca. 2 cm^{-1} and an integration time spanning from 100 to 400 s for the spectral region of 400-1800 cm^{-1}.

3. Results and discussion

3.1 Physico-chemical characteristic of nanoparticles

The three different samples of TiO_2, designated as T_R (rutile), $T_{A/R}$ (anatase/rutile), T_A (anatase) having different proportion of crystalline phase were chosen and thoroughly characterized (Table 1).

Table 1. Physico-chemical characterization

Sample	Crystalline Phase	Purity	Surface area BET (m^2/g)	Primary particles dimension (nm)	Hydrodynamic size (nm)	PCZ	ζ Potential (pH 7.4)
T_R	100% Rutile	>99.5	39	Lenght 40.5 ± 12.1 [a] Diameter 27.4 ± 6.5 [a]	156 PDI 0.12	5.5	-35.7
$T_{A/R}$	77% Anatase 23% Rutile	>99.6	53	19±3 [b] 45±7 [b]	214 PDI 0.18	6.9	-13.2
T_A	100% Anatase	>99.6	83	11±2 [b]	428 PDI 0.38	6.7	-17.5

a. Evaluated by TEM
b. Evaluated by XRD in according to the Scherrer's equation

The degree of purity of the TiO_2 samples evaluated by X-rays fluorescence (XRF) was found to be very high (>99%). The samples showed a different specific surface area which correspond to a different nanostructure (Table 1). In fact, the estimated crystallites size of anatase was lower than in the other two samples, in agreement with to the higher SSA value obtained.

The size analysis of the NP aggregates has been obtained by DLS in water at pH 10. At this pH value the particles exhibit a highly negative surface charge which minimize the formation of agglomerates because of electrostatic repulsions among particles. All samples exhibited aggregates having a wide range of diameters as suggested by the high polydispersity index (PDI) values (Table 1). The anatase sample appears to be composed by aggregates larger than the other two samples.

In water the TiO_2 NP surface is charged due to the the presence of dissociated hydroxyl groups and partially uncoordinated $Ti^{(IV)}$ ions [23]. The charge depends upon the pH value of the suspension and may be estimated by the evaluation of the ζ potential, i.e. the potential across the double layer of ions around the particles.

The variation of the ζ potential of the samples as a function of pH in deionised water is reported in Figure 1A. Under these experimental conditions, the point of zero charge (PZC) of T_R (5.5) resulted to be different from the PZC of the other two samples (6.7 and 6.9 respectively) suggesting a higher acidity of the hydroxyl groups in rutile. The other two samples exhibit a similar behavior according with the prevalence of the anatase phase in the $T_{A/R}$ sample.

The ζ potential was also measured by suspending the powders in phosphate buffer (PBS) (Figure 1B) as the interaction with proteins has been measured in PBS to simulate physiological conditions

(see below). A decrease in ζ potential values was observed in the whole pH range as a consequence of the high ionic strength of the suspension. Furthermore, a dramatic shift of the PZC was observed for all samples. This effect may be due to a strong adsorption of phosphate ions at the surface. Interestingly the ζ potential at physiological pH appears nearly the same for the three samples, suggesting that, in physiological conditions, the differences observed in water among rutile and anatase disappear thus the electrostatic interactions with proteins are expected to be similar for the two phases.

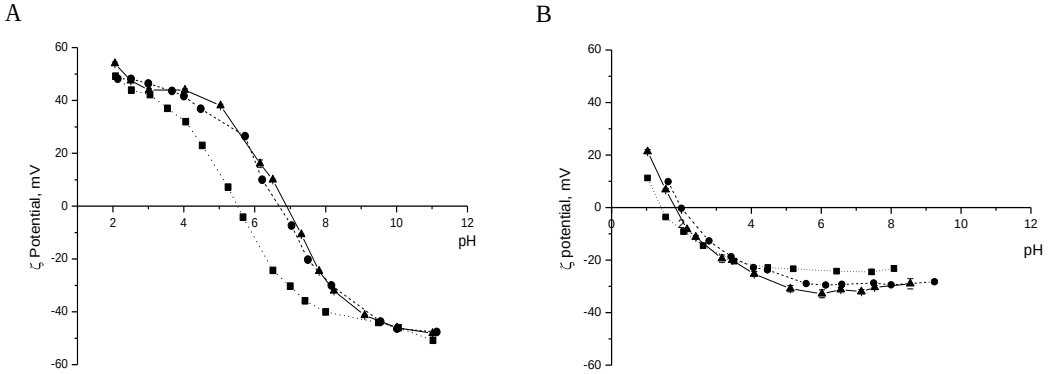

Figure 1 Variation of ζ Potential of TiO_2 samples measured in different dispersant. The curves are measured after the suspension of samples nanoparticles T_R (dot), $T_{A/R}$ (solid), T_A (dash) in water (A) and PBS (B) by sonication. The acquisition of these curve is repeated for three times.

3.2 Evaluation of the amount of protein interacting with nanoparticles

To investigate the affinity of the proteins for the TiO_2 buffered solutions of BSA or BPF at increasing concentration (500-10000 mg/L) were incubated for 1 hour with the powders. The amount of protein interacting with the particles was calculated by the decrease of their concentration in the supernatant after incubation. The results are reported in Figure 2 and are expressed as amount of protein adsorbed on TiO_2 per unit surface area *vs* the final concentration of the protein in solution after adsorption. The amount of adsorbed protein corresponding to a theoretical monolayer on an ideal flat surface, considering a side-on adsorption, is also reported in the graph (dotted line).

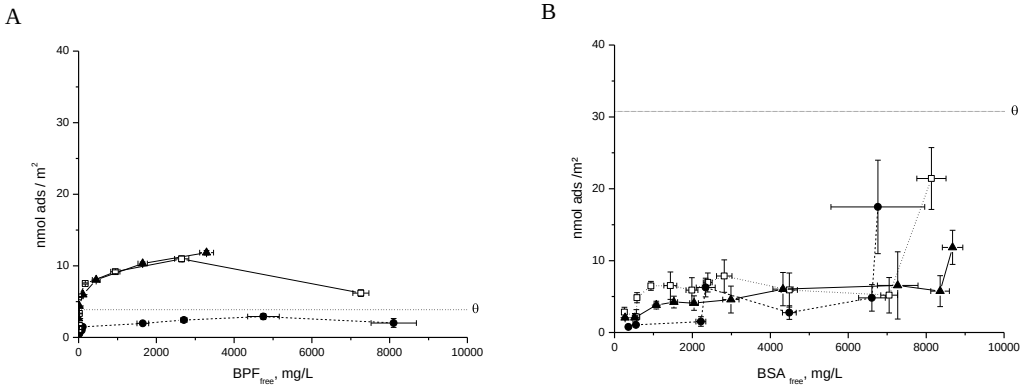

Figure 2 Comparisons of protein adsorption curves. The quantity of adsorbed fibrinogen (A) and albumin (B) on titania samples T_R squares), $T_{A/R}$ (triangles), T_A (circles) is show. The theoretical monolayer (θ) is not reached for all titania samples after the adsorption of BSA, while in the case of BPF the adsorption on $T_{A/R}$ and T_R largely exceeds of the θ.

BSA (Figure 2B) interacted with the three samples in a similar manner since the three adsorption curves appear close to each other. The amount of interacting protein increased with the protein concentration and reached a plateau at values lower than the theoretical monolayer. A different behavior was observed for BPF (Figure 2A). A rapid initial growth of the amount of protein adsorbed with a very low residual protein concentration was observed. The amount of protein adsorbed increased and overcame at high coverage, the theoretical monolayer.

The amount of fibrinogen adsorbed on T_R nanoparticles results to be similar to $T_{A/R}$ sample while a different behavior was observed for the anatase which accommodates a lower amount of proteins on its surface.

The data obtained suggest that fibrinogen has an affinity for TiO_2 surface higher than albumin. Differences in the properties of the two proteins may account for such differentiation. Both proteins have a negative net charge at pH 7.4 and therefore the adsorption of the proteins occurs against the repulsive electrostatic forces with the negative TiO_2 surface. However, BSA exposes at the solvent in the native form a largely uniform negative charge. Repulsive forces act both against the adsorption onto the surface but also laterally among proteins which are therefore unable to adsorb close to each other to form a compact monolayer. Conversely fibrinogen has a negatively charge domain in the central region, but the αC regions, exhibit a positive net charge due to the presence of arginine and lysine [13]. The presence of these positive domains possibly allows orientating the protein thus facilitating the adsorption onto negative surfaces and the formation of multi-layers.

The anatase sample exhibits a lower capacity to absorb proteins. This effect was much more evident for BPF than for BSA. Since in PBS the ζ potential of the three samples was similar such differences are not expected to be due to a different contribution of the electrostatic forces. On the other hand the anatase sample exhibits primary particles smaller than the other two samples, which are organized in large aggregates. The presence of pores among particles accessible to nitrogen but not to fibrinogen may be one reason of the lower amount of protein interacting with this sample. On the other hand, the lower primary particle size and, consequently, the higher curvature of each single primary particle makes rougher the surface of the aggregates possibly lowering the number of possible points of interaction with fibrinogen. In the case of BSA, this effect is expected to be less important being BSA a much smaller molecule.

3.3 Evaluation of the extent of coverage of the NPs surface.

To get insight on the extent of the coverage of the surface the shift of ζ potential following protein adsorption was also evaluated.

One of the most relevant effects of the formation of the protein corona on NPs is the consequent masking of the NP surface. Being charged entities proteins are expected to modify the ζ potential of the NPs. We therefore measured the ζ potential shift of the titania powders, $T_{A/R,}$ previously incubated with the fibrinogen and albumin at different concentrations (Figure 3A and B respectively). Similar results were obtained with the other two powders (data not shown).

The adsorption of BPF led to a shift of the PZC toward the isoelectric point of the proteins, suggesting that the coverage of the surface increased proportionally with protein concentration (Figure 3A) in agreement with the adsorption curve. However, the isoelectric point (pI) of the protein was not reached even at high coverage suggesting that the particle surface was still exposed at the solvent. This was expected for BSA, since the amount absorbed was not enough to fully cover the surface. However a PZC lower than pI was also observed for BPF. A preferential orientation of the protein at the surface with the positive side toward the surface may account for this result.

A similar masking effect is expected to occur with the protein corona is formed by both proteins reversibly or irreversibly interacting with the surface. Therefore the data obtained did not give any information on the reversibility of the process. This information is important to predict the behavior of proteins in competitive conditions.

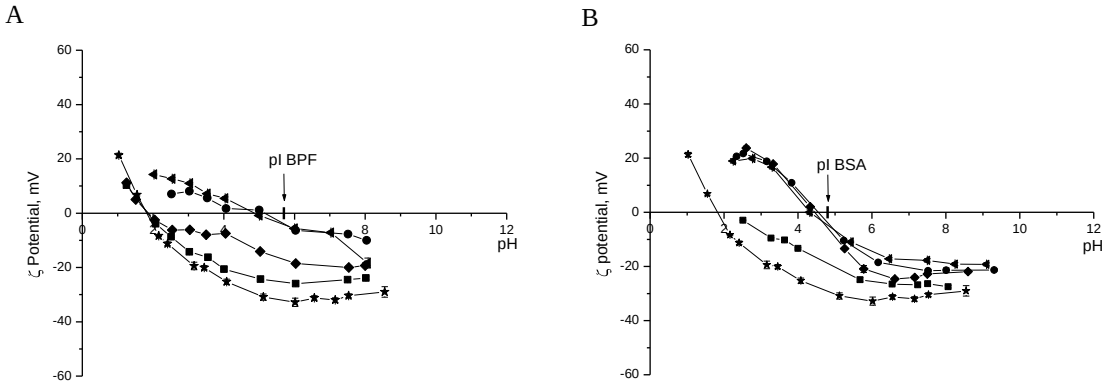

Figure 3 Variation of ζ potential after protein adsorption. Increasing concentration of fibrinogen (A) and albumin (B) is associated with the shift of the nanoparticles point of zero charge(PZC) toward the protein isoelectric point (pI). The curves are relative to $T_{A/R}$ sample before (stars) and after incubation with different protein concentration 10 (triangles), 5 (circles), 2.5 (diamonds) and 0.5 (squares) g/L.

3.4 Evaluation of reversibility

The reversibly-bound fraction of the protein corona is expected to be removed by applying a negative protein concentration gradient, i.e. re-suspending the protein –NP conjugates in a fresh protein-free buffer. If the protein corona is totally reversible, the ζ potential of the NPs is expected to shift back to the values observed for the free NP surface. On the contrary, if a totally irreversible corona is formed upon NP surface subsequent washing will not modify the conjugate ζ potential. In Figure 4 the ζ potential curves measured after suspending $T_{A/R}$ previously incubated with the proteins in PBS are reported. BPF appeared to interact irreversibly with TiO_2 nanoparticles since no shift of the ζ potential curves was observed (Figure 4A). Similar results were obtained with the other two powders (data not shown). Also for albumin the interaction appeared almost irreversible (Figure 4B).

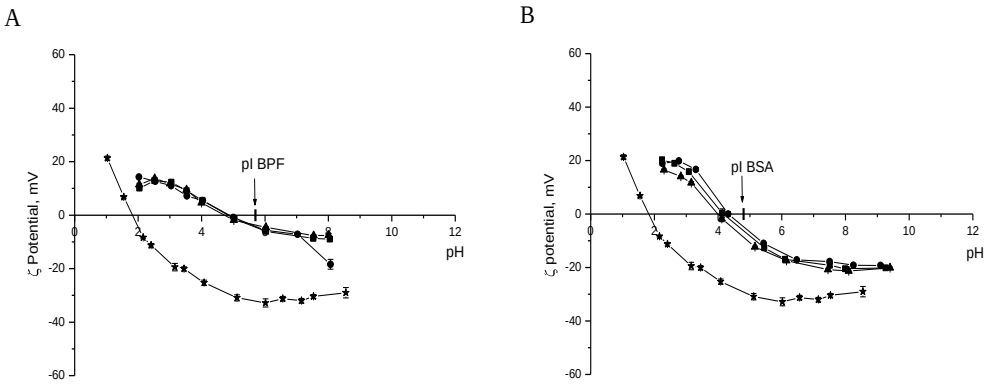

Figure 4 Variation of ζ potential after washing. The curves are acquired for the sample before the adsorption (stars), after the incubation with a high (10000 mg/L) protein concentration (circles), one cycle (squares) and three cycles of washing (triangles). This experiment has been carried out also for the other nanoparticles and for two other protein concentrations (5000 and 500 mg/L) and in all cases the adsorption resulted to be irreversible**.**

3.5 Evaluation of surface-driven protein conformational changes with Raman Spectroscopy

Albumin and fibrinogen are both soft proteins and their adsorption on nanoparticles is irreversible. It is therefore to be expected that BSA and BPF interacting with TiO_2 NPs, undergo some kind of conformational change. The evaluation of such conformational changes may be studied with micro-Raman spectroscopy. Raman spectroscopy can be used to evaluated the protein secondary structure by analyzing the vibrational frequencies of the bands associated with the backbone amide bonds that are dependent upon the secondary arrangement of the polypeptide chain [24].

The amide I band corresponds to the sum of coupled modes of the polypeptide backbone. A major contribution to the amide I modes comes from the C-O stretching of the peptide carbonyl groups [25]. It is possible to evaluate the surface-driven conformational modifications by comparing the Raman spectral pattern of the native folded protein with that of the same protein adsorbed on the titania surface. Note that the Raman modes of both anatase and rutile TiO_2 are located in the region between 200 and 800 cm^{-1} and therefore no interference by these picks is expected. The spectra of BSA are acquired in the native form or adsorbed on the titania nanoparticles; the spectra relative to the interaction with the $T_{A/R}$ sample are reported in Figure 5. The amide I Raman bands for the intensity maximum of each Raman spectrum was normalized to 1. The amide I band of native BSA (Figure 5, black spectrum, 1657 cm^{-1}) is slightly shifted toward higher wavenumbers (1660 cm^{-1}) when BSA is adsorbed on $T_{A/R}$, and the amide III band (1278 cm^{-1}) is slightly shifted toward lower wavenumbers (1267 cm^{-1}) after the adsorption. These shifts are typical of a protein conformational change; it is possible that these modifications in protein structure are due to oxidative damage linked with the reactivity (photocatalitic activity) of titania samples [26]. The three peaks of aromatic residues (1557, 1588, and 1618 cm^{-1}) are assigned according to previous data. [24, 25].

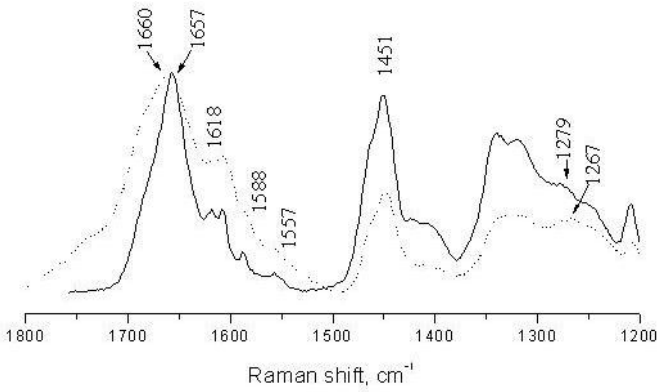

Figure 5 Evaluation of protein conformational change after adsorption on $T_{A/R}$ Raman spectra of BSA native (solid spectra) and adsorbed on nanoparticles (dot spectra).These data are the average of ten acquisition. The arrows point the peak of amide I (1657 cm^{-1}) and amide III (1279 cm^{-1}) bands. The shift of these bands is typical of a conformational change. Spectra intensities were normalized to amide I peak.

4. Conclusions

In this study, the interaction of albumin and fibrinogen with three samples of TiO_2 having distinct crystal phases and different primary particle size, has been evaluated.

We found that both albumin and fibrinogen interact irreversibly with the negative surface of TiO_2 NPs. The interaction with albumin appears to be driven by conformational changes of the protein at the surface. This was expected since BSA has a low resistance to deformation. In the case of BPF both conformational changes and electrostatic forces between TiO_2 surface and the positive domains of the proteins my account for such interaction. Fibrinogen interacts in large quantity with T_{AR} and T_R while a lower amount was observed in the case of the anatase sample. This effect was likely due to a lower availability of the surface to the large fibrinogen molecule and to the higher roughness of this

sample as a consequence of the lower dimension of the primary particles, while the differences in surface properties related to the crystal phase seemed to play a minor role. A smaller effect was observed for BSA because this protein may closely contact the particles surface while BPF is expected to "see" the TiO_2 powders as rough aggregates (Figure 6).

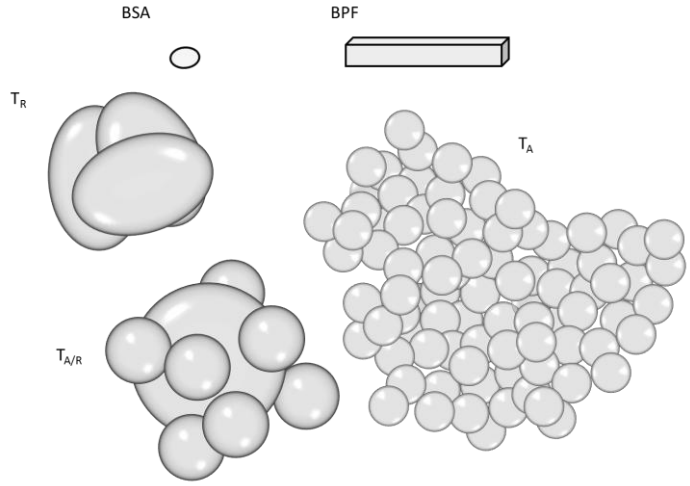

Figure 6 Proteins and titania nanoparticles. Schematic representation

It is well known that small proteins are faster to diffuse and then arrive at the surface before large proteins. The early formed protein corona is however expected to evolve: in fact proteins having higher affinity for surfaces like fibrinogen may replace smaller proteins through a mechanism known as Vroman's effect [17, 27, 20]. The present data suggest that the surface curvature of particles may modulate the amount of fibrinogen interacting with the nanoparticles and possibly its affinity for the surface. Since the interaction of fibrinogen with NPs has been shown to trigger inflammatory responses [16] the lower affinity of fibrinogen for the sample having smaller primary particles may correspond to a possible higher biocompatibility of small TiO_2 nanoparticles.

References

[1] Oberdörster G *et al* 2009 Nanoparticles and the Brain: Cause for Concern? *Journal of nanoscience and nanotechnology* **9** pp4996-5007
[2] Savolainen K *et al* 2010 Risk assessment of engineered nanomaterials and nanotechnologies *Toxicology* **269** pp 92-104
[3] Schrurs F and Lison D 2012 Focusing the research effort *Nature nanotechnology* **7** pp 546-548
[4] Pietroiusti A 2012 Health implications of engineered nanomaterials *Nanoscale* **4** pp1231-1247
[5] Lin W *et al* 2006 In vitro toxicity of silica nanoparticles in human lung cancer cells *Toxicology and applied pharmacology* **217** pp 252-259
[6] Fubini B *et al* 2010 Physico-chemical features of engineered nanoparticles relevant to their toxicity *Nanotoxicology* **4** pp 347-363
[7] Schulze C *et al* 2011 Interaction of metal oxide nanoparticles with lung surfactant protein A *European Journal of pharmaceutics and biopharmaceutics* **77** pp 376-383
[8] Lundqvist M *et al* 2008 Nanoparticle size and surface properties determine the protein corona with possible implications for biological impacts *Pnas* **105** pp 14265-14270
[9] Walczyk D *et al* 2010 What the Cell "Sees" in Bionanoscience *Journal of the American Chemical Society* **132** pp 5761-5768

[10] Lynch I *et al* 2007 The nanoparticle - protein complex as a biological entity; a complex fluids and surface science challenge for the 21st century *Advances in Colloid and Interface Science* **134-35** pp 167-174.
[11] Kamali P P and Simberg D 2011 Interaction of nanoparticles with plasma proteins: implication on clearance and toxicity of drug delivery systems *Expert opinion drug delivery* **8** pp 343-357
[12] Sugio S *et al* 1999 Crystal structure of human serum albumin at 2.5 Å resolution *Protein engineering* **12** pp 439-446
[13] Jung SY *et al* 2003 The Vroman effect:a molecular level description of fibrinogen displacement *Journal american chemical society* **125** pp 12782-12786
[14] Jackson S P 2007 The growing complexity of platelet aggregation *Blood* **109** pp 5087-5094
[15] Thevenot P *et al* 2008 Surface chemistry influences implant biocompatibility *Current Topics in Medicinal Chemistry* **8** pp 270-280
[16] Deng ZJ *et al* 2011 Nanoparticle-induced unfolding of fibrinogen promotes Mac-1 receptor activation and inflammation *Nature nanotechnology* **6** pp 39-44
[17] Nel A *et al* 2009 Understanding biophysicochemical interactions at the nano-biointerface *Nature Materials* **8** pp 543-557
[18] Nel A *et al* 2006 Toxic potential of materials at the nanolevel *Science* **311** pp 622-627
[19] Rivera Gil P *et al* 2010 Correlating physico-chemical with toxicological properties of nanoparticles: the present and the future *Acs Nano* **4** pp 5527-5531
[20] Fenoglio I *et al* 2011 Multiple aspects of the interaction of biomacromolecules with inorganic surfaces *Advanced Drug Delivery Reviews* **63** pp 1186-1209
[21] Liu H *et al* 2007 Nanomedicine for implants: A review of studies and necessary experimental tools *Biomaterials* **28** pp 354-369
[22] Bolis V *et al* 2012 Hydrophilic/hydrophobic features of TiO_2 nanoparticles as a function of crystal phase, surface area and coating, in relation to their potential toxicity in peripheral nervous system *Journal of colloid and interface science* **369** pp 28-39
[23] Suttiponparnit K *et al* 2011 Role of surface area primary particle size and crystal phase on titanium dioxide nanoparticles dispersion properties *Nanoscale research letters* **6**
[24] Turci F *et al* 2010 An integrated approach to the study of the interaction between proteins and nanoparticles *Langmuir* **26** pp 8336-8346
[25] Strehle M A *et al* 2004 a raman spectroscopy study of the adsorption of fibronectin and fibrinogen on titanium dioxide nanoparticles *Phys. Chem. Chem. Phys*. **6** pp 5232-5236
[26] Fenoglio *et al* 2009 Non-Uv-induced radical reactions at the surface of TiO_2 nanoparticles that may trigger toxic responses *chem. Eur. J.* **15** pp 4614-4621
[27] Vroman L 1962 Effect of absorbed proteins on the wettability of hydrophilic and hydrophobic solids *Nature* **196** pp 476-7